Proceedings of the 2002 IEEE/RSJ
Intl. Conference on Intelligent Robots and Systems
EPFL, Lausanne, Switzerland • October 2002

Hybrid Architecture for Simultaneous Localization and Map Building in Large Outdoor Areas

Favio Masson†, Jose Guivant‡, Eduardo Nebot‡

† *Universidad Nacional del Sur, Departamento de Ingenieria Electrica*
‡ *Australian Centre for Field Robotics / CMTE, Sydney, Australia*

Abstract

This paper address the problem of navigating in very large outdoor unstructured environments. It presents solutions to the problem of closing large loops in simultaneous localization and map building applications. A hybrid architecture is presented that make use of the Extended Kalman Filter to perform SLAM in an efficient form and a Monte Carlo type filter to resolve the data association problem present when closing large loops. The proposed algorithm incorporates integrity to the standard SLAM algorithms by allowing multimode distribution to be handled in real time. Experimental results in outdoor environments are also presented.

1 Introduction

Reliable autonomous navigation in highly unstructured outdoor environments presents formidable problems in terms of sensing, perception and navigation algorithms [1]. The problem of localization given a map of the environment or estimating the map knowing the vehicle position is known to be a solved problem and in fact applied in many research and industrial applications [2] [3]. Outdoor environments present additional challenges due to the lack of reliable sensors and perception algorithm that can work reliable under all weather conditions.

A much more complicate problem is when both, the map and the vehicle position have to be estimated. This problem is usually referred as Simultaneous Localization and Map Building (SLAM) [4] or Concurrent Map Building and Localization (CML) [5]. This problem has been addressed in [6] using a Monte Carlo method in indoor problems and in [7] using sum of Gaussian in a sub-sea applications. Although these methods can handle multimodal distributions they are still computationally expensive for real time applications.

The Kalman Filter can be extended to solve the SLAM problem [4], once appropriate models for the vehicle and sensors are obtained. In [9] the real time implementation aspects of SLAM using EKF techniques were addressed. A Compressed Extended Kalman Filter (CEKF) algorithm was introduced that significantly reduces the computational requirement without introducing any penalties in the accuracy of the results. Sub-optimal simplification were also presented in [10] to update the full covariance matrix of the states bounding the computational cost and memory requirements.

Simultaneous navigation and map building algorithms are based on a exploration stage and re-visit of known places to register the new learned map to the known map. Depending on the quality of the kinematics models and external sensors used the exploration stage can be extended to larger areas. Nevertheless no matter how good sensors and models are, at one point the accumulated error will make the registration task impossible. This problem is shown in Figure 1. In this experimental run the vehicle started near point labeled 3 and circulated in CW direction. The Figure shows the estimated path using a CEKF filter aided with absolute GPS information [11]. The stars represents natural landmarks incorporated as features into the map. The vehicle uses dead reckoning information to predict its position and incorporates features into the map to bound the dead-reckoning errors. If the vehicle return to the point 3 with an error smaller than the separation between landmarks then it is possible to use standard algorithm to perform data association and register the new learned local map. In this particular case there are very few landmarks in the part of the trajectory labeled 1-2-3 making the estimated vehicle error to grow to 10 meters when returning close to the initial position labeled 3. This error is plotted as an ellipse in the Figure 1. Since the separation between the landmarks A and B are approximately 8 meters the system will not be able to perform the data association and will be in failure.

This is an inherent limitation of all simultaneous navigation and mapping methods and is independent of

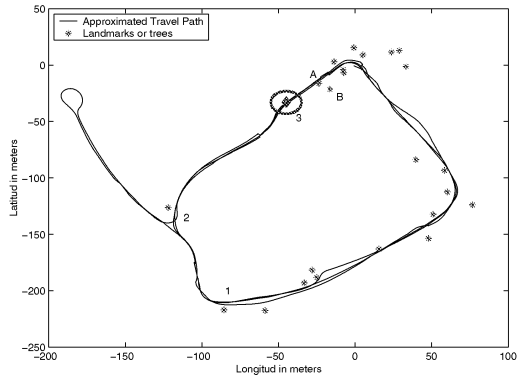

Figure 1: *Closing the loop in a large environment with few features*

the implementation method or model used. In this paper a robust solution to this problem is presented using a combination of the CEKF with a Monte Carlo Filter. This hybrid architecture is designed to exploit the efficiency of the CEKF algorithm to estimate and maintain vehicle and map states and to provide appropriate initialization to the Monte Carlo filter to accelerate the convergence of the particle type filters once a possible data association problem is detected. The algorithms are presented for generic range/bearing sensors and can be extended to bearing only and range only sensors.

The paper is organized as follows. Section 2 presents the Bayes framework and in particular the Particle Filter implementation. Section 3 presents the main result of this paper that is the hybrid architecture proposed with the CEKF and the Particle Filter. Section 4 presents experimental results in outdoor unstructured environments. Finally Section 5 presents conclusions.

2 Bayesian Estimation in navigation problems

The SLAM problem under a probabilistic estimation approach requires that the marginal probability density $p(x_{L_k}, \mathbf{m}|\mathbf{Z}^k, \mathbf{U}^k, x_0)$ must be known for all k, where x_{L_k} is the vehicle state, x_0 its initial condition, $\mathbf{m}$ are the states representing a feature in the map and $\mathbf{Z}^k$ and $\mathbf{U}^k$ are the observations and input signals respectively at time k. To obtain the recursively form of this density [7] [8], it is assumed that the density $p(x_{L_{k-1}}, \mathbf{m}|\mathbf{Z}^{k-1}, \mathbf{U}^{k-1}, x_0)$ is known. Then applying the Bayesian rule and the Total Probability theorem we have

$$p(x_{L_k}, \mathbf{m}|\mathbf{Z}^k, \mathbf{U}^k, x_0) = \kappa p(z_k|x_{L_k}, \mathbf{m}) \int p(x_{L_k}|x_{L_{k-1}}, u_k) p(x_{L_{k-1}}, \mathbf{m}|\mathbf{Z}^{k-1}, \mathbf{U}^{k-1}, x_0) dx_{L_{k-1}} \quad (1)$$

where κ is a normalization constant, $p(z_k|x_{L_k}, \mathbf{m})$ represents the observation model and $p(x_{L_k}|x_{L_{k-1}}, u_k)$ models the vehicle dynamic. When the map m is known

$$p(x_{L_k}|\mathbf{m}, \mathbf{Z}^k, \mathbf{U}^k, x_0) = \kappa p(z_k|\mathbf{m}, x_{L_k}) \int p(x_{L_k}|x_{L_{k-1}}, u_k) p(x_{L_{k-1}}|\mathbf{m}, \mathbf{Z}^{k-1}, \mathbf{U}^{k-1}, x_0) dx_{L_{k-1}} \quad (2)$$

represents the *Localization Problem.*

2.1 Localization with the Particle Filter

Particle Filters approximate the joint posterior probability density with a set of random samples called particles. As the number of samples becomes large, they provide an exact, equivalent representation of the required distribution, that is the filter output will be close to the Bayesian filter. In this work we use the SIR (Sampling Importance Resampling) filter [12], to localize a vehicle in a predefined map using range and bearing information. Assuming that R samples $\{x^i_{k-1}\}^R_{i=1}$ of the previous posterior distribution are available, the process model is then used to propagate these samples to obtain $\{\tilde{x}^i_k\}^R_{i=1}$. The new samples represents the *a priori* probability density $p(x_k|\mathbf{m}, \mathbf{Z}^{k-1}, \mathbf{U}^k, x_0)$.

The update stage is performed in two steps. The first step consist of the evaluation likelihood for each predicted particle as,

$$w_i = \frac{p(z_k|\mathbf{m}, \tilde{x}^i_k)}{\sum_{j=1}^{R} p(z_k|\mathbf{m}, \tilde{x}^j_k)} \quad (3)$$

where z_k is the observation at time k. The pair $\{\tilde{x}^i_k\}^R_{i=1}$, $\{w^i_k\}^R_{i=1}$ defines a discrete distribution that tends to the real continuous *posterior* distribution as R tends to infinity.

The second stage performs a resampling selecting only the particles with probability $p_r\{x^j_k = \tilde{x}^i_k\} = w^i_k$ for each j. Algorithms that perform this stage with computational complexity $\propto R^2$ and $\propto R$ can be found in [12] and [13] respectively.

Finally the probability of measuring z_k given the estate $\tilde{x}_k$ is required, that is $p(z_k|\mathbf{m}, \tilde{x}^i_k)$.

Calculation of $p(z_k|\mathbf{m}, x_{L_k})$**.** In the case of range and bearing observation (z_r, z_β), it can be assumed that the measurements are contaminated by additive noise (γ_r, γ_β) with a general probability distribution. The conditional probability distribution of the observation (z_r, z_β) respect to the vehicle states, considering the uncertainty in the landmark position and the observation noise can be obtained from the following integral,

$$p(z_k|\mathbf{m}, x_{L_k}) = \int_{\Omega} p(\mathbf{m}_x, \mathbf{m}_y, \gamma_r, \gamma_\beta)\ \mu\ |\overrightarrow{dS}| \qquad \Omega = \{(\mathbf{m}_x, \mathbf{m}_y, \gamma_r, \gamma_\beta) \in \Re^4\} \tag{4}$$

The integral is a surface integral and $p(\mathbf{m}_x, \mathbf{m}_y, \gamma_r, \gamma_\beta)$ is the joint probability density distribution of the random variables due to the four noise sources. The factor $\mu \cdot |\overrightarrow{dS}|$ is the surface differential used to perform the integration over the surface region defined by the equality constrains given in equation 5.

$$\begin{aligned} z_r &= \sqrt{(\mathbf{m}_x - x_L)^2 + (\mathbf{m}_y - y_L)^2} + \gamma_r \\ z_\beta &= \arctan(\tfrac{\mathbf{m}_y - y_L}{\mathbf{m}_x - x_L}) - \varphi + \tfrac{\pi}{2} + \gamma_\beta \end{aligned} \tag{5}$$

The probability density distribution 4 can be evaluated using the probability density distribution restricted to the observations,

$$p_{z_r, z_\beta}(z_{r_0}, z_{\beta_0}) = \frac{\partial F_{z_r, z_\beta}(z_{r_0}, z_{\beta_0})}{\partial z_r \partial z_\beta} \tag{6}$$

where $F_{z_r, z_\beta}(z_{r_0}, z_{\beta_0})$ is the probability distribution. After some manipulations this distribution can be expressed as

$$\begin{aligned} &F_{z_r, z_\beta}(z_{r_0}, z_{\beta_0}) = \\ &\int_{-\infty}^{\infty}\int_{-\infty}^{\infty}\int_{-\infty}^{\gamma_{r_0}}\int_{-\infty}^{\gamma_{r_0}} p(\mathbf{m}_x, \mathbf{m}_y, \gamma_r, \gamma_\beta) \cdot d\gamma_r \cdot d\gamma_\beta \cdot d\mathbf{m}_x \cdot d\mathbf{m}_y \\ &\gamma_{r_0} = z_{r_0} - \sqrt{(m_x - x_L)^2 + (m_y - y_L)^2}, \\ &\gamma_{\beta_0} = z_{\beta_0} - \arctan(\tfrac{m_y - y_L}{m_x - x_L}) + \varphi - \tfrac{\pi}{2}, \end{aligned} \tag{7}$$

The integral argument is the probability density distribution of the four random variables,

$$p(\mathbf{m}_x, \mathbf{m}_y, \gamma_r, \gamma_\beta) = p_{\mathbf{m}_x, \mathbf{m}_y, \gamma_r, \gamma_\beta}(\mathbf{m}_x, \mathbf{m}_y, \gamma_r, \gamma_\beta) \tag{8}$$

Finally, the probability density distribution is the derivative of the probability distribution,

$$\begin{aligned} &p_{z_r, z_\beta}(z_{r_0}, z_{\beta_0}) = \tfrac{\partial F_{z_r, z_\beta}(z_{r_0}, z_{\beta_0})}{\partial z_r \partial z_\beta} = \\ &\int_{-\infty}^{\infty}\int_{-\infty}^{\infty} p(\mathbf{m}_x, \mathbf{m}_y, \gamma_{r_0}(\mathbf{m}_x, \mathbf{m}_y), \gamma_{\beta_0}(\mathbf{m}_x, \mathbf{m}_y)) d\mathbf{m}_x d\mathbf{m}_y \end{aligned} \tag{9}$$

This integral is numerically evaluated reducing the integration region to the $\mathbf{m}_x, \mathbf{m}_y$ space close to the landmarks. This simplification is valid provided that the pdf $p_{\mathbf{m}_x, \mathbf{m}_y}(\mathbf{m}_x, \mathbf{m}_y)$ is approximated by a sum of gaussians pdf's (SOG). In this work a region of size 2σ deviation centered at the expected position of the landmark is used. The density probability distribution $p_{\mathbf{m}_x, \mathbf{m}_y}(\mathbf{m}_x, \mathbf{m}_y)$ then becomes negligible outside these regions.

3 Compressed filter and the aided of the bootstrap filter

The Compressed Extended Kalman Filter (CEKF) [9], is an implementation of the Extended Kalman Filter that presents significant computational advantages to various type of systems and in particular to SLAM problems. In [10] a suboptimal solution to reduce the computational and memory requirements to $\propto N$ is also presented. Still there are very important problems to address when applying these algorithms in large environments as stated in the introduction of this paper. This approach generates state estimations with mono-modal probability distributions, that is not capable of handling multimodal probability distributions. These situations are typical when closing large loops, that is revisiting known places after a significant exploration period. It is at this stage where the standard data association methods usually fail. A particle filter can address this problem since it naturally deals with multi-hypothesis problems.

The proposed architecture uses CEKF under normal conditions to perform SLAM. At a certain time the system may not be able to perform the association task due to large errors in vehicle pose estimation. This is an indication that the filter can not continue working with a mono-modal probability density distribution. At this point, we have the CEKF estimated mean and deviation of the states representing the vehicle pose and landmark positions. With the actual map a de-correlated map is built using a coordinate transform and the decorrelation procedures presented in [10]. A particle filter uses this information to resolve the position of the rover as a localization problem. When the multi-hypothesis are resolved the CEKF is restarted with the back propagated states values. Then the CEKF remains in operation until a new potential data association problem is detected.

3.1 Practical implementation

This subsection presents several important implementation issues that need to be taken into account to maximize the performance of the proposed architecture.

Map for the particle filter. The SLAM algorithm builds a map while vehicle explore a new area. The map states will be, in most cases, highly correlated in a local area. In order to use the particle filter to solve the localization problem a two dimensional map probability density distribution needs to be synthesized from a completely originally strongly correlated n dimension map. The decorrelation procedure is implemented in two steps. The map, originally represented in global coordinates in now represented in a local frame referenced to two beacons states that are highly correlated to all the local landmarks. The local landmarks that are not base are then referenced to this new base. This result in a covariance matrix of the form,

$$p\mathbf{m} = \begin{bmatrix} \mathrm{p}_{\mathbf{m}_1} & C_{12} & \cdots & C_{1m} \\ C_{21} & \mathrm{p}_{\mathbf{m}_2} & \cdots & \vdots \\ \vdots & \ddots & \ddots & \vdots \\ C_{m1} & \cdots & \ddots & \mathrm{p}_{\mathbf{m}_m} \end{bmatrix} \tag{10}$$

where the cross-correlation components between states of different landmarks are usually weak, i.e. they meet the condition $C_{i,j}/\sqrt{p_{m_i} \cdot p_{m_j}} << 1$. To de-correlate the map it is necessary to apply an additional step. A conservative bound matrix for (eq. 10) can be easily obtained increasing the diagonal components and deleting the cross-correlation terms. This can be implemented as shown in eq 11 where $diag[\cdot]$ represents the elements of a diagonal matrix [10]. For presentation purposes, all the states in equation 11 are assumed to belong to different landmarks. The decorrelation procedure performs the decorrelation of block diagonal matrices, being each block diagonal matrix the covariance of the states representing a particular landmark.

$$\tilde{p}\mathbf{m} = diag \begin{bmatrix} p\mathbf{m}_1 + \sum_{j}^{j \neq 1} \mid k_{1j} \cdot C_{1j} \mid \\ \vdots \\ p\mathbf{m}_m + \sum_{j}^{j \neq m} \mid k_{mj} \cdot C_{mj} \mid \end{bmatrix} \tag{11}$$

The set $\{k_{ij}\}_{i,j}$ meets the condition $k_{ij} = 1/k_{ji} > 0$. This *un-correlated* map is used to define a two dimension map probability density distribution used by the particle filter to localize the vehicle.

Initialization of the filter. As the number of particles affects both, the computational requirements and convergence of the algorithm, its necessary to select an appropriate set of particles to represent the a priori density function at time T_0. Since the particle filters work with samples of a distribution rather than its analytic expression it is possible to select the samples based on the most probable initial pose of the rover. A good initial distribution is a set of particles that is dense in at least a small sub-region

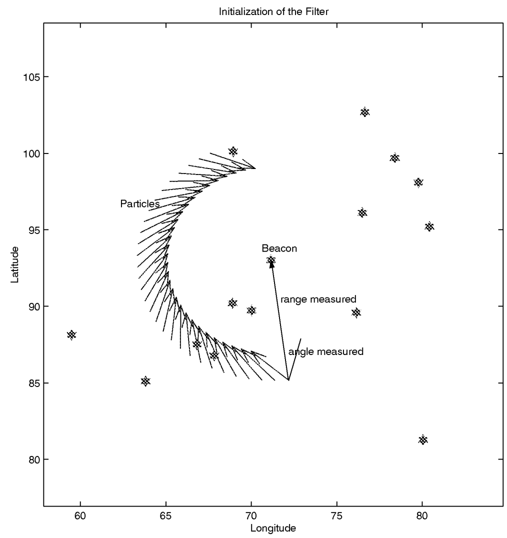

Figure 2: *Helix conformation with one measure and one beacon ($z_\beta = 47.75°$, $z_r = 7.85m$)*

that contains the true states value. The initial distribution should be based in at least one observation in a sub-region that contains this true states value.

Once a range and bearing from a landmark is obtained a distribution is created having a shape similar to a family of solid helical cylinders. Each helix centre corresponds to a hypothetical landmark position with its radio defined by the range observation (Figure 2). The helical cylinder section can be adjusted by evaluating its sensitivity to the noise sources $\gamma_{x_i}, \gamma_{y_i}, \gamma_r, \gamma_\beta$.

Although it is recognized that some returns will not be due to landmarks, all range and bearing observations in a single scan are used to build the initial distribution. Even though a family of families of helices will introduce more particles than a single family of helices (one observation), it will be more robust in presence of spurious observations. Considering the observations of range and bearing as perfect observations, this defines a discontinued one dimensional curve (family of helices), C, in the three dimensional space (x, y, φ)

$$C = \bigcup_{i=1}^{N} C_i$$

$$C_i = \left\{ (x, y, \varphi) \setminus \begin{array}{l} x = x(\tau) = x_i + z_r \cdot \cos(\tau) \\ y = y(\tau) = y_i + z_r \cdot \sin(\tau) \\ \varphi = \varphi(\tau) = \tau - z_\beta - \frac{\pi}{2} \\ \tau \in [0, 2\pi) \end{array} \right\} \tag{12}$$

Assuming the presence of noise in the observation

$$\begin{array}{c} z_r = z_r^* + \gamma_r, \;\; z_\beta = z_\beta^* + \gamma_\beta \\ x_i = x_i^* + \gamma_{x_i}, \;\; y_i = y_i^* + \gamma_{y_i} \end{array} \tag{13}$$

Figure 3: Experimental run in an outdoor environment

This family of helices becomes a family of cylindrical regions surrounding the helices. This helices regions can be restricted by considering the expected value and deviation of φ. They can be used to reduce the bounds of τ variation.

Interface with the CEKF. Two main issues need to be addressed to implement the switching strategy between the CEKF and the SIR filter. The first problem involves the detection of the potential data association failure while running the CEKF. This is implemented in this work by monitoring the estimated error in vehicle and local map states. The second issue is the reliable determination that the particle filter has resolved the multi-hypothesis problem and is ready to send the correct position to the CEKF back propagating its results. This problem is addressed by analyzing the evolution of the estimated deviations errors. The filter is assumed to converge when the estimated standard deviation error becomes less than two times the the noise in the propagation error model for x, y and φ. The convergence of the filter is guarantee by the fact that the weights (eq. 3) are bounded above at any instant of time [14]. These weights are obtained from the integral 9. This integral is always different from zero since it is calculated over distribution that is zero only in $\pm\infty$ making the weights to be bounded by 1.

4 Experimental Results

This section presents experimental results of the proposed hybrid architecture running in an unstructured environment shown in Figure 3. In this case trees are used as the most relevant features to build a navigation map [11]. The CEKF filter is used to navigate when no potential data association fault are detected.

When a potential data association failure is detected the particle is initialized with the uncertainty and position reported by CEKF filter and is run after convergence is reached. The results of the experimental run are shown in Figures 4 to 6. The upper left corner of Figure 5 shows the initialization of the particle filter for the case when range and bearing are used. This Figure clearly shows the helix shape of the initial distributions. The arrows represent the position and orientation of the vehicle and the stars the beacons present in the map. Figure 4 shows the average magnitude of the position of the mobile across a Monte Carlo simulation consisting of 50 runs (thin continuous line). The stars are natural landmarks incorporated into the map by the CEKF (see Guivant et. all [4]). The dotted line is the differential GPS position taken as a reference to verify the operation of the filter. The vehicle started from the left down corner of the Figure 4. In the initial part of the trajectory the mean is not useful due to the multi-hypothesis nature of the distribution at this time. This can be seen in Figure 5 where the estimated path is represented for one run at selected times. In this case the clouds of particles shows the convergence of the filter.

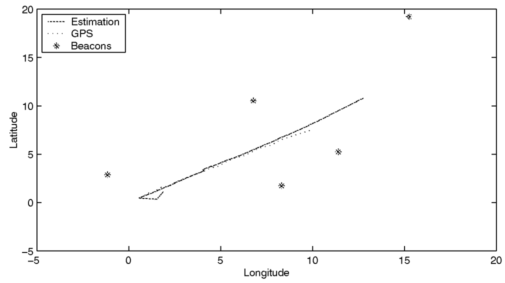

Figure 4: Average magnitude of the position of the mobile across a Monte Carlo simulation consisting of 50 runs for the case of a range and bearing sensor

Figure 6 shows the deviations of the states x and y of the vehicle averaged over the fifty runs of the Monte Carlo simulation. It is clear that the convergence of the filter is achieved with the observations present in the first laser scan since the error is reduced during a single time stamp. The error at time 26 decreased from 2.2 to 0.5 meters. This scan included observation to several beacons. It is important to note that although the environment can be crowded with landmarks and other spurious objects the algorithm remains robust since no data association is performed at this stage.

5 Conclusions

This paper presented a hybrid architecture that make use of the Compressed Extended Kalman Filter (CEKF) algorithm to perform SLAM in an efficient

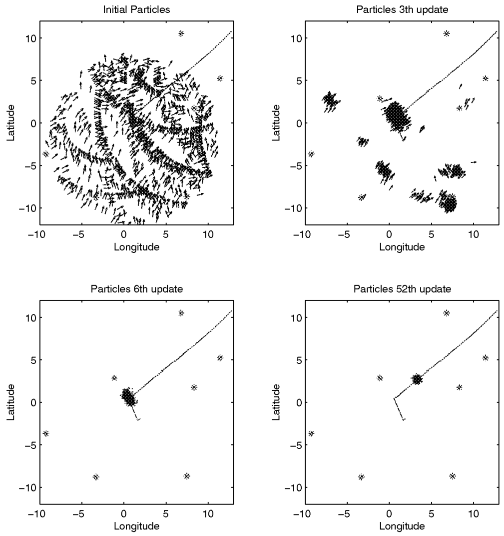

Figure 5: *GPS position and particles cloud after processing a number of observations: Top (left to right): Initialization and after 3 observations. Bottom (left to right): After 6 and 52 observations.*

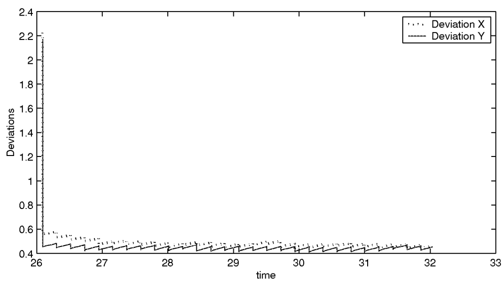

Figure 6: *History of state's x and y error when the filter is run with range and bearing information*

form and a Monte Carlo type filter to resolve the data association problem present when closing large loops. The experimental results have shown that this approach can be used to increase the integrity of EKF based systems by providing the capability to handle multi-mode distributions.

Three factors affect the computational requirements and convergence of the algorithm. The initialization, the number of particles and the number of beacons that can be measured in a laser scan.

It was shown that a good initialization is essential to assure the convergence of the algorithm with a given number of particles. In all runs performed using range and bearing information the filter managed to resolve the multi-hypothesis in only one laser scan. This results can be extrapolated to the case of bearing only information and range only information. Research in underway to address the other two issues.

References

[1] R. Chatila, *Autonomous navigation in natural environments*, Robotics and Autonomous Systems, 16 (1995), pp. 197–211.

[2] A. Elfes, *Occupancy Grids: A probabilistic framework for robot perception and navigation*, ph. d. thesis, Department of Electrical Engineering, Carnegie Mellon University, 1989.

[3] H. F. Durrant-Whyte, *An autonomous guided vehicle for cargo handling applications*, Int. Journal of Robotics Research, 15 (1996), pp. 407–441.

[4] J. Guivant, E. Nebot, and H. Durrant-Whyte, *Simultaneous localization and map building using natural features in outdoor environments*, Proc. IAS-6 Intelligent Autonomous Systems, (2000), pp. 581–586.

[5] J. Leonard, P. Neuman, and R. Rikoski, *Towards robust data association and feature modelling for concurrent mapping and localization*, International Symposium of Robotics Research, (2001). Lorne, Australia.

[6] S. Thrun, W. Bugard, and D. Fox, *A Real Time Algorithm for Mobile Robot Mapping with Applications to Multi-Robot and 3D Mapping* , Proc. Of 2000 IEEE, San Francisco, (2000), pp. 321–326.

[7] H. Durrant-White, S. Majumder, S. Thrun, M. D. Battista, and S. Scheding, *A bayesian algorithm for simultaneous localization and map building*, International Symposium of Robotics Research, (2001). Lorne, Australia.

[8] D. Fox, W. Burgard, and S. Thrun, *Markov localization for mobile robots in dynamic environments*, Journal of Art. Int. Research, 18 (1999), pp. 391–427.

[9] J. Guivant and E. Nebot, *Optimization of the simultaneous localization and map building algorithm for real time implementation*, IEEE Trans. on Robotics and Automation, Vol 17, June (2001), pp. 242–257.

[10] J. Guivant and E. Nebot, *Improved computational and memory requeriments of simultaneous localization and map building algorithms*, IEEE ICRA 2002, pp. 2731–2736.

[11] J. Guivant, F. Masson, and E. Nebot, *Simultaneous localization and map building using natural features and absolute information*, Robotics and Autonomous Systems, (to appear).

[12] N. J. Gordon, D. J. Salmond, and A. F. M. Simth, *Novel approach to nonlinear/non-gaussian bayesian state estimation*, IEE Proceedings-F, 140 (1993), pp. 107–113.

[13] J. Carpenter, P. Clifford, and P. Fearnhead, *Improved filter for nonlinear problems*, IEE Proceedings on Radar, Sonar Navigation, 146 (1999), pp. 2–7.

[14] D. Crisan and A. Doucet, *Convergence of sequential monte carlo methods*, tech. report, Technical Report Cambridge University, CUED/FINFENG /TR381, 2000.